

# FIXED HEAD KINEMATIC PILE BENDING MOMENT: ARTIFICIAL NEURAL NETWORK APPROACH

<sup>1</sup>Ahmad Irshad, <sup>2</sup>M. Hesham El Naggari, <sup>1</sup>Akhtar Naeem Khan

## ABSTRACT

This paper deals with the application of Artificial Neural Network (ANN) to estimate elastic kinematic seismic bending moment at pile head in end bearing piles embedded in homogeneous soil layer overlying bed rock which is subjected to harmonic excitation. The data generated for training and testing the ANN models is based on **Beam on Dynamic Winkler Formulation**. Two ANN models are developed, namely ANN1 and ANN2. ANN1 predicts the pile head moment when bed rock is excited by natural frequency of the overlying soil deposit. ANN2 is applicable to excitations with any frequency. The inputs to ANN1 are the length to diameter ratio of pile and ratio of the elastic modulus of pile to that of soil. The inputs to ANN2 also include the frequency ratios. The output of ANN models is the normalized pile head bending moment. Feed forward Levenberg-Marquardt back propagation algorithm is used to train the ANN models. To evaluate the performance of the ANN models, correlation coefficients and coefficient of variation of the ratio of predicted to target response with reference to unity as mean are used.

Both the ANN models mapped the target response to a reasonable accuracy, and show a promising application in the area of seismic soil pile structure interaction. The ANN models developed in this study can, therefore, be used in practice for preliminary design purposes to estimate pile head moment with little effort of calculations in a hand held programmable calculator.

## KEY WORDS

artificial neural network, pile, kinematic moment, winkler model

## INTRODUCTION

The passage of seismic waves in soil imposes curvatures, and thereby bending moments in the pile along its length. The magnitude of this moment can be sometimes quite high and shall be evaluated as part of any dynamic soil pile structure interaction problem (Irshad A. & Akhtar N.K. 2006, Mizuno, H. 1987).

For fixed head piles embedded in homogenous soils, the kinematic bending moment are high at the fixed end of pile, particularly at frequencies near the fundamental frequency of the soil deposit. A situation of particular importance occurs when the predominant frequency of the seismic input matches the natural frequency of soil deposit. In such cases, the kinematic bending moment at fixed head of pile may be larger than the

---

<sup>1</sup> Professor, Department of Civil Engineering, NWFP University of Engineering and Technology Peshawar, Pakistan

<sup>2</sup> Professor, Department of Civil and Environmental Engineering, University of Western Ontario, London, Ontario N6A 5B9

inertial bending moment, especially when the natural frequency of the supported structure is far from the seismic input predominant frequency.

Amongst the simplest techniques to find kinematic pile response is the Beam on Dynamic Winkler Formulation which necessitates carrying out free field site response analysis; imposing free field displacement time histories on winkler supports to excite the pile; and carrying out dynamic analysis to find the response of pile. In this paper Artificial Neural Network is used for function approximation to estimate normalized fixed pile head moment ( $M_n$ ) due to kinematic interaction. Two ANN models are developed in this paper. The first model, ANN1 estimates  $M_n$  when pile base is excited by the fundamental frequency of the overlying soil deposit. The second model, ANN2 is applicable for a range of excitation frequencies. Feed forward Levenberg-Marquardt back propagation algorithm is used to train the ANN models. Using the trained ANN model, the kinematic bending moment of a fixed head pile can be estimated without performing any dynamic analysis.

### PARAMETERS OF SEISMIC SOIL PILE INTERACTION

Figure 1 shows the layout of the pile soil system considered in this study. The fixed head pile rests on rock formation, which is considered as a hinged support. The bedrock is excited by vertically propagating S-waves characterized by a harmonic displacement of  $u_g(t) = U_g e^{i\omega t}$ , where  $U_g$  is the ground displacement amplitude and  $\omega$  is the excitation circular frequency. The pile group effect is not considered as it plays a negligible role in kinematic interaction (Gazetas et al., 1992).

Beam on Dynamic Winkler Formulation (BDWF) is adopted in this paper to generate data for ANN models training. The ranges of input parameters selected to generate data for ANN1 and ANN2 are given in Table 1. The considered ranges cover most of the practical situations.

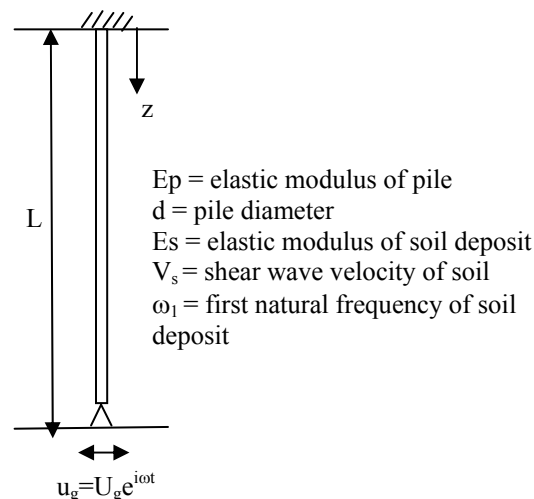


Figure 1: Pile Soil System

Table 1: Ranges of Parameters used for data generation

Parameter	Minimum	Maximum	Increment	Data points
$E_p/E_1$	100	9600	500	20
$L/d$	10	40	2.5	13
Frequency ratio $\alpha = \omega d/V_s$	0.01	0.8	0.01	80
Total data (ANN1)				260
Total data (ANN2)				20800

**BEAM-ON-DYNAMIC-WINKLER-FOUNDATION (BDWF) MODEL**

Data for ANN models was generated by modeling the soil pile system as BDWF, which is schematically shown in Figure 2. The pile is connected to free field soil along its length by continuously distributed linear springs ( $k_x$ ) and dashpots ( $c_x$ ) that resist the lateral pile motion. The support of the springs and dashpots are excited by the free field displacement  $u_{ff}(z,t)$ .

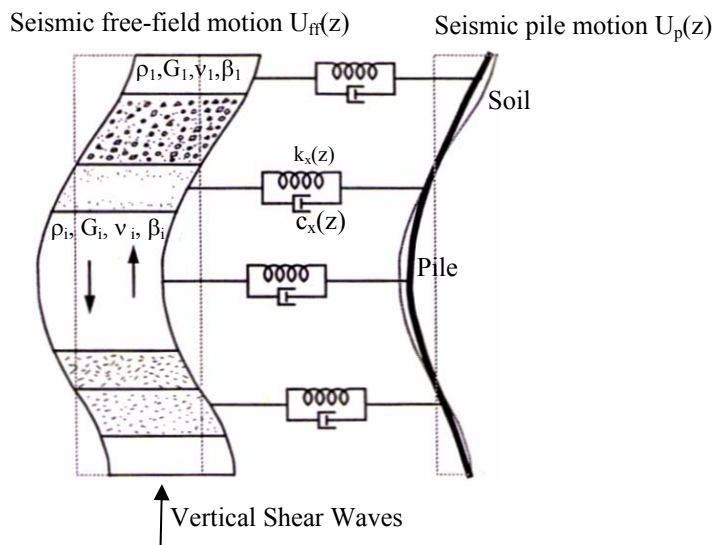


Figure 2: Beam-On-Dynamic-Winkler Foundation model

**Sprin Stiffness  $k_x$**

The spring stiffnesses in this study are adopted from M. Kavvadas and G. Gazetas (1993). Thus  $k_x = \delta E_s$  where  $E_s$  soil modulus of elasticity of soil and  $\nu$  soil poisson's ratio.

$$\delta = \frac{2}{1-\nu^2} \left( \frac{E_s d^4}{E_p I_p} \right) \left( \frac{L}{d} \right)^{1/8}$$

### Dashpot coefficients $c_x$

During soil pile interaction, the seismic energy is dissipated through hysteretic (material damping) and radiation (geometric damping). The former incorporates the internal energy dissipation in the soil, and is, thus related to soil damping ratio,  $\beta_s$  and the later is a geometric effect and represents the radiation of energy by waves spreading geometrically away from the pile soil interface. Hence the distributed dashpot/length of pile is,  $c_x = c_r + c_m$ , where  $c_r =$  distributed radiation dashpot coefficient and  $c_m =$  distributed material dashpot coefficient.

In this study these coefficients are adopted from Gazetas, G. & Dobry, R. (1984a,b).

$$c_m = \frac{2k_x \beta_s}{\omega}$$

$$c_r = 2d\rho_s V_s \left(1 + \left(\frac{V_c}{V_s}\right)^{\frac{5}{4}}\right) a_0^{-\frac{1}{4}}$$

Where  $V_c$  is the apparent velocity of the extension compression waves taken as the Lysmer's analog velocity  $V_{La}$  and  $V_s$  is the shear wave velocity of soil under consideration.

$V_c = V_{La} = \frac{3.4V_s}{\pi(1-u)}$  at all depths except near the ground surface ( $z \leq 2.5d$ ), where three-dimensional effects arising from the stress-free boundary are better reproduced by use of  $V_c \cong V_s$

### Solution of differential equation governing kinematic response of piles

The governing differential equation for harmonic excitation  $u_{g(t)}$  at the bed rock is

$$\hat{U}_{pp}''''(z) - \lambda^4 \hat{U}_{pp}(z) = \alpha \hat{U}_{ff}(z), \text{ where}$$

$$\lambda^4 = \frac{m_p \omega^2 - S_x}{E_p I_p}, \alpha = \frac{S_x}{E_p I_p}, S_x = K_x + i c_x \omega$$

$S_x$  is complex impedance function.  $\hat{U}_{ff}(z)$  and  $\hat{U}_{pp}(z)$  are displacement amplitudes of free field and pile at depth  $z$  respectively and hyphen over them in above differential equation represents differential with respect to depth  $z$ .

Equation has the general solution

$$\hat{U}_{pp}(z) = [e^{-\lambda z} e^{\lambda z} e^{-i\lambda z} e^{i\lambda z}] \begin{Bmatrix} D1 \\ D2 \\ D3 \\ D4 \end{Bmatrix} + s \hat{U}_{ff}(z)$$

$$s = \frac{\alpha}{q^{*4} - \lambda^4}, \text{ where } q^* \text{ is complex wave number} = \sqrt{\frac{\omega}{V_s + i\beta_s}}$$

$D1, D2, D3,$  and  $D4$  are arbitrary constants to be evaluated through boundary conditions.

### Boundary Conditions

The boundary conditions suggest that rotation and shear at top of pile are zero i.e.  $\theta(0,t)=0$ ,  $V(0,t)=0$ , respectively and moment at pile base is zero,  $M(L,t)=0$ ; and pile displacement at base is equal to ground displacement at bed rock i.e.  $u_p(L,t)=u_g(t)$ .

The solution of the differential equation is implemented in MATLAB environment as a general case for a single homogeneous soil layer to make it robust for parametric study. The code first evaluates the free field displacements as a function of depth, their first, second, and third derivative. Determine four arbitrary constants through four boundary conditions and then evaluates normalized pile head bending moment  $M_n = M/(\rho_p \omega^2 d^4)$ , where  $M$  is the pile head bending moment, and  $\rho_p$  is the pile density.

### ARTIFICIAL NEURAL NETWORK (ANN) MODEL

#### ARCHITECTURE OF ANN MODEL FOR ESTIMATING PILE HEAD MOMENT

ANNs are data processing paradigms constructed of highly interconnected nodes (neurons) that map a complex input pattern with a complex output pattern (Dowla, F.U. and Rogers, L.L. 1995, Hagan, M.T., Demuth, H.B., and Beale, M. 1996). A Levenberg–Marquardt back-propagation algorithm was used in this research. It is one of the fastest methods available for training moderate-sized feed-forward neural networks (Hagan, M.T., Demuth, H.B., and Beale, M. 1996). The theory and implementation of the Levenberg-Marquardt algorithm is given in detail by (More, J.J. 1977). The architecture of ANN1 model consisting of an input layer of two input neurons, a hidden layer of two neurons, and an output layer consisting of one output neuron is shown in Figure-1. The symbols  $w$  and  $b$  in figure 3 represent connection and bias weights with subscripts representing the corresponding neurons between two layers.

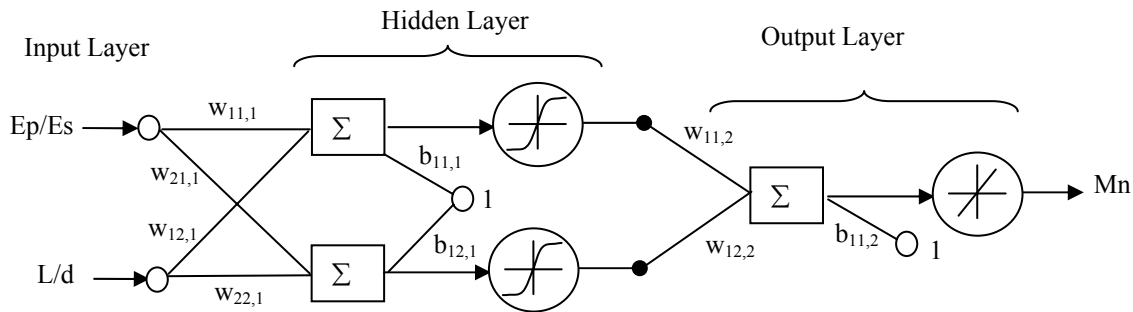


Figure:3 Artificial Neural Network Architecture for ANN1

For the ANN models developed in this study a tan–sigmoid (the hyperbolic tangent) transfer function is used for the hidden layer neurons, and a linear transfer function is used for the output neuron. This structure is found to be useful for function approximation (or regression) problem under present study.

The ANN1 model works on two inputs i.e.  $Ep/Es$  and  $L/d$  while ANN2 model uses four inputs  $Ep/Es$ ,  $L/d$ ,  $ao$ , and  $\omega/\omega_1$ , and therefore have two and four neurons respectively in the input layers. The output of the ANN models is the normalized pile

head moment (Mn) and therefore has only one output neuron. The number of neurons in the hidden layer was determined by training several networks with different numbers of hidden neurons and comparing the predicted results with the desired output. In this study, two to ten neurons were considered for both ANN models. Optimum numbers of neurons were found to be two and eight respectively for ANN1 and ANN2. These neurons avoid underfitting i.e large training and testing errors and prevent overfitting i.e. low training error but high testing error.

### TRAINING AND TESTING ARTIFICIAL NEURAL NETWORK MODEL

In the training phase of ANN model, the network is supplied with a set of inputs and known target values. The network adjusts the connection weights and bias such as to reduce the error between the known target and network output. Once the connections weights are established that ensure minimum training error, the next phase is the testing phase in which the network is presented with examples that are new to the network. The network predicts the output using the connection weights and biases established in the training phase.

The data generated to train ANN1 and ANN2 are first randomized and then divided into two sets namely the training data set and the testing data set. The data was so divided so as to give comparable statistical properties for training and testing (Table 2). Seventy percent (70%) of the available data was used for training and 30% was reserved for testing.

Table 2. Statistical Properties of Training, and Testing Data for ANN2 and ANN1 (shown in parenthesis)

Data Type	Statistical Properties	Input and Output Parameters				
		Ep/Es	L/d	ao	$\omega/\omega_1$	Mn
Training Data	Maximum	9600 (9600)	40 (40)	0.01	20.37	6083.2 (6134)
	Minimum	100 (100)	10 (10)	0.80	0.0637	0.654 (63.9)
	Range	9500 (9500)	30 (30)	0.79	20.3	6082.5 (6070)
	Mean	4830 (4894)	25 (24.8)	0.40	6.47	292.2 (3096)
	Standard Deviation	2887.7 (2822.6)	9.35 (9.3)	0.23	4.62	567.7 (1777)
Testing Data	Maximum	9600 (9600)	40 (40)	0.01	20.37	6123.7 (6132)
	Minimum	100 (100)	10 (10)	0.8	0.0637	0.654 (63.9)
	Range	9500 (9500)	30 (30)	0.79	20.30	6123 (6068)
	mean	4896 (4747)	24.87 (25.4)	0.40	6.379	308.7 (2998)
	Standard Deviation	2872.5 (3053.7)	9.34(9.56)	0.23	4.58	598.6 (1919.2)

Preprocessing of the training data is performed so that the processed data was in the range of -1 to +1. In this study the training data sets (inputs and targets outputs) are scaled (preprocessed) according to

$$\mathbf{Pn} = 2 \times \frac{(\mathbf{P} - \mathbf{minP})}{(\mathbf{maxP} - \mathbf{minP})} - 1 \quad (1)$$

$$\mathbf{Tn} = 2 \times \frac{(\mathbf{T} - \mathbf{minT})}{(\mathbf{maxT} - \mathbf{minT})} - 1 \quad (2)$$

P = matrix of the input vectors; T= matrix of the output vectors; Pn=matrix of scaled input vectors; Tn= matrix of scaled target output vectors; minP= vector containing minimum values of the original input; maxP = vector containing maximum values of the original input; minT = vector containing the minimum value of the target output ( i.e. minimum value of Mn in the training dataset); maxT = vector containing the maximum value of the target output ( i.e. maximum value of Mn in the training dataset). The scaled data was then used to train the neural network. The data from the output neuron have to be postprocessed to convert the data back into unscaled units to get actual Mn value according to

$$\mathbf{T} = 0.5 \times (\mathbf{Tn} + 1)(\mathbf{maxT} - \mathbf{minT}) + \mathbf{minT} \quad (3)$$

The preprocessing and postprocessing parameters are given in Table 3.

Table 3: Pre- and Post-processing Parameters for ANN2 and ANN1 (in parenthesis)

	<b>Ep/Es1</b>	<b>L/d</b>	<b>ao</b>	<b>w/w1</b>	<b>Mn(max)</b>
<b>Minimum</b>	100 (100)	10 (10)	0.01	0.0637	0.6641 (63.92)
<b>Maximum</b>	9600 (9600)	40 (40)	0.80	20.4	6083.2 (6133.9)

The training was carried out until the average sum squared error over all the training patterns was minimized. This occurred after about 1000 cycles of training. The connection and bias weights obtained after ANN training can be used to estimate the Mn.

#### PROCEDURE FOR ESTIMATING PILE HEAD MOMENT

The ANN model described in this paper can be used to predict the Mn. The procedure can easily be programmed into a computer, or performed using a calculator capable of performing simple matrix operations. The input data is first preprocessed according to equation-1 to get scaled input vector **Pn**.

The Mn is then obtained through the network as follows:

$$\mathbf{Tn} = [\mathbf{W}_2 \times \{ \tanh(\mathbf{W}_1 \times \mathbf{Pn} + \mathbf{B}_1) \} + \mathbf{B}_2] \quad (4)$$

Where **Tn** = matrix of scaled output vector and

$\mathbf{W}_1$ = weight matrix representing connection weights between the input layer neurons and hidden layer;  $\mathbf{W}_2$ = weight matrix representing connection weights between the hidden layer neurons and the output neuron;  $\mathbf{B}_1$ =bias vector for the hidden layer neurons;  $\mathbf{B}_2$ = bias vector for the output layer neuron.

The scaled output **Tn** is then unscaled using equation-3 to obtain Mn.

### ANN MODEL PREDICTION

In order to evaluate the capability of the ANN model, the model was presented with new data that was not part of the training data set and the  $M_n$  calculated. The correlation coefficient (R) and coefficients of variation (cv) of the ratio  $M_n$  (BDWF) to  $M_n$ (ANNs) with reference to unity as mean are given in table-4. It is seen that the prediction of ANN1 model is superior to ANN2 model. This is due to the fact that the response is quite sensitive to the frequency of excitation, being grossly reduced at high  $\omega/\omega_1$  ratios. However, from practical point of view, the ANN2 estimation of  $M_n$  is quite satisfactory because the error term is larger at low moments which occur at high  $\omega/\omega_1$  ratios. The contribution of these high modes to actual seismic input signal will be quite low.

Table 4: Prediction Parameters of ANN1 and ANN2

ANN Model	Testing Data		Training Data		Complete Data	
	cv(%)	R	cv(%)	R	cv(%)	R
ANN1	3.1	0.99	3.3	0.99	3.26	0.99
ANN2	16.5	0.99	16.2	0.99	16.3	0.99

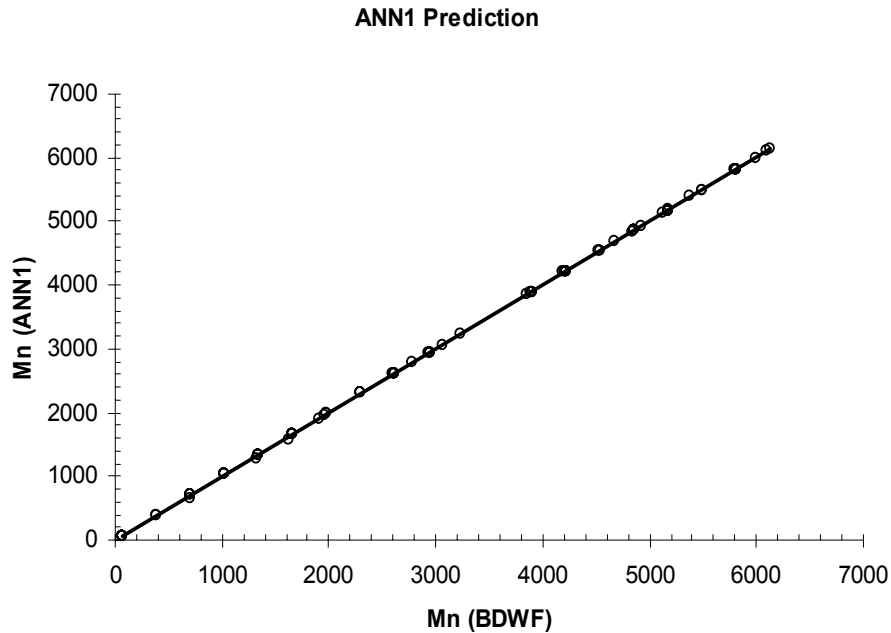


Figure 4: ANN1 model prediction

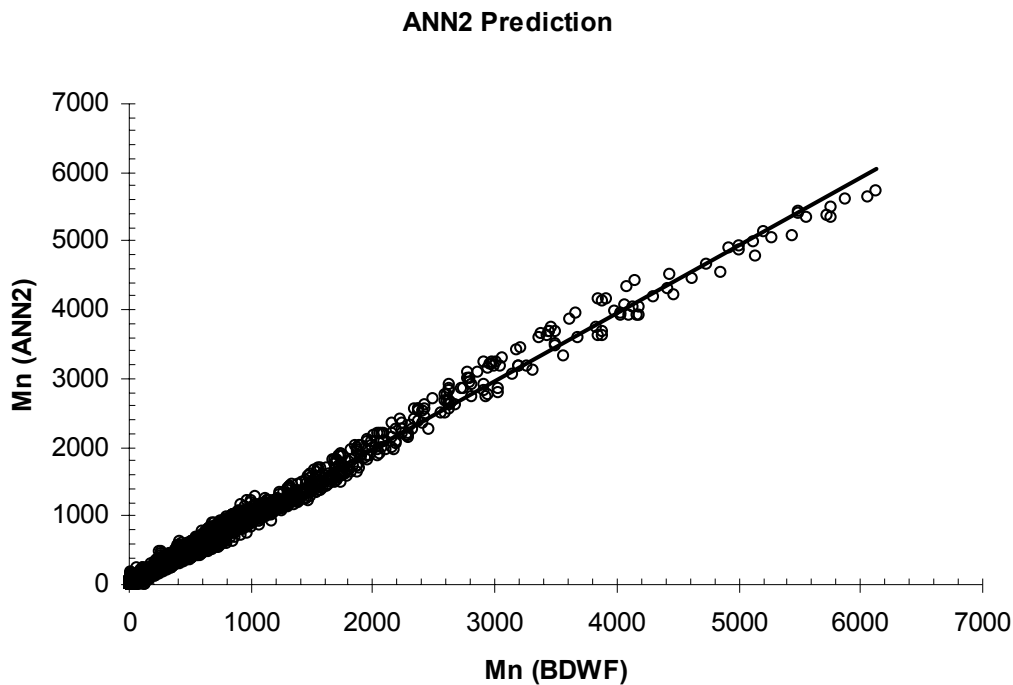


Figure 5: ANN2 model prediction

## CONCLUSION

The ANN models used in this paper have performed quite satisfactorily and have potential to be used for more complex seismic soil pile structure interaction problems with more complex configuration of the neural network architecture. The ANN model if used to simulate the closed form solutions can drastically reduce the amount of calculations involved and can give quite satisfactory results, at least for preliminary design purposes. It has the advantage that it can be implemented in simple hand calculator capable of matrix operation.

Secondly, if real data of dynamic soil pile structure interaction is available either on prototype or model, the ANN can evaluate the complex response coupling the nonlinear parameters, which are otherwise difficult to numerically model.

## REFERENCES

- Dowla, F.U. and Rogers, L.L. (1995). "Solving problems in environmental engineering and geoscience with artificial neural networks", MIT, Cambridge, Ma.
- Gazetas, G. & Dobry, R. (1984a). "Horizontal response of piles in layered soils" J. Geotech. Engng Div. Am. Soc. Civ. Engrs. 110, No.1,20-40.

- Gazetas, G. & Dobry, R. (1984b). "Simple radiation damping model for piles and footings. Horizontal response of piles in layered soils". *J. Geotech. Engng Div. Am. Soc. Civ. Engrs.* 110, No.6, 937-956.
- Gazetas, G. K. Fan, T. Tazoh, K. Shimizu, M. Kavvadas, and N. Makris (1992). "Seismic Pile-Group-Structure Interaction. Piles Under Dynamic Loads" *Geotechnical Special Publication No.34* pp.56-93.
- Hagan, M.T., Demuth, H.B., and Beale, M. (1996) "Neural Network design", PWS, Boston.
- Irshad A., & Akhtar N.K. (2006). "Kinematic Seismic Response of Piles- Importance and Modeling" *GeoCongress 2006: Geotechnical Engineering in the information Technology Age*.
- Kavvadas M. and G. Gazetas (1993), "Kinematic seismic response and bending of free-head piles in layered soil" *Geotechnique* 43, No.2, 207-222.
- More, J.J. (1977), "The Levenberg-Marquardt algorithm: Implementation and theory.", *Numerical Analysis*, Watson, G.A. ed., Springer, Heidelberg, 105-116.
- Mizuno, H. (1987). "Pile damage during earthquakes in Japan" *Dynamic Response of Pile Foundations* (ed. T. Nogami), pp. 53-78. New York: American Society of Civil Engineers.